LA-UR-91- 2706

LA-UR--91-2706

DE91 018034

Los Alamos National Laboratory is operated by the University of California for the United States Department of Energy under contract W 7405 ENG 36

TITLE: ACCELERATOR DRIVEN NEUTRON SOURCES FOR FUSION-MATERIALS TESTING

AUTHOR(S): G. P LAWRENCE

SUBMITTED TO: JOURNAL OF FUSION ENERGY (PROCEEDINGS OF FUSION POWER ASSOCIATES ANNUAL MEETING AND SYMPOSIUM, PRINCETON, NJ, JUNE 25-26, 1991.)

Los Alamos National Laboratory
Los Alamos, New Mexico 87545

FORM NO 836 R4
ST NO 2629 5/91

DISCLAIMER

Accelerator-Driven Neutron Sources for Fusion-Materials Testing *

G. P. Lawrence
Los Alamos National Laboratory
Los Alamos, NM 87545

Introduction

Several accelerator driven neutron sources have been proposed for satisfying the requirements of a high flux high-volume international fusion materials testing facility that could be built in the near future. This paper summarizes the features and projected performance for the three accelerator sources that are leading candidates for such a role and that are viewed by the International Energy Agency (IEA) as worthy of further evaluation. These are: 1) the d-Li source, in which 35-MeV deuteron beams are incident on flowing lithium targets, 2) the t-H_2O source, in which 21 MeV triton beams strike high-speed water jets, and 3) the Spallation source in which a 600-MeV proton beam bombards a heavy metal target. Each of these sources attempt to meet the evaluation criteria developed by the international fusion-materials research community in a recent worshop,[1] which are:

- Neutron flux: At least 2 MW/m^2 to simulate demo-reactor conditions. Accelerated testing calls for 10 MW/m^2 or greater
- Spectrum: As close as possible to that in a fusion reactor first wall. Spectral tailoring should be possible.
- Fluence: Demo relevant fluences (100 dpa, 10 MW yr/m^2), with high source availability (> 70%).
- Volume: A 10 liter test volume is required in region of neutron flux > 2 MW/m^2 (0.9 x 10^{18}n/cm^2 s).
- Gradient: Flux gradients should be < 10%/cm.
- Accessibility: Test volume must allow easy changeout of experimental assemblies.
- Time structure: A quasi continuous neutron flux is mandatory.

Deuterium-Lithium Neutron Source

In the Deuterium Lithium (d-Li)[2] neutron source concept, 35 MeV deuterons incident on a lithium jet target generate a fusion-like spectrum from the Li(d,n) reactions. Much of the relevant technology was developed by the FMIT program in the early 1980s.[3] Although not implemented, FMIT was to provide a 100 mA D$^+$ beam to a single lithium jet target, generating a 0.5 liter test volume exposed to a flux of 10^{18} n · m^{-2} · s^{-1}, and a 0.01 liter volume at 10^{19} n · m^{-2} · s^{-1}. Flux gradients were relatively steep because of the strong forward peaking of the neutron yield.

* Work performed under the auspices of the U.S. Department of Energy, Office of Fusion Energy, by Los Alamos National Laboratory

Recently a Los Alamos group has proposed an improved D-Li source concept [2] that employs linac technology advances to supply higher beam currents than FMIT, and that uses a two-target/two-beam configuration to provide larger test volumes at a given neutron flux as well as lower flux gradients. The reference scheme, sketched in Fig. 1, consists of two D^+ accelerator modules, each delivering a 250-mA continuous wave (cw) beam to two lithium jet targets oriented at a relative angle of 90°. An initial step in a staged deployment might consist of a single 250-mA (or lower current) module, with the output beam split and transported to two targets. As implied in the sketch, the total D^+ current could ultimately be expanded to 1000 mA.

Figure 1 tabulates energy, current, frequency, and radio-frequency power in the different accelerator sections of the D-Li source driver. Other parameters are listed in Table 1. Preliminary beam simulations and accelerating structure designs were done to predict beam performance and power consumption. Structure frequencies are considerably higher than in FMIT, allowing a compact accelerator and improved beam quality. A 1-MW cw 350 MHz RF source is available to drive the drift tube linac (DTL). The high energy beam transport (HEBT) in each module incorporates a cavity that increases the beam energy spread to 1.0 MeV (rms) and an octupole magnet that flattens and widens the transverse beam distribution. At the target the beam distribution is Gaussian (1 cm rms) along the jet flow, while in the cross flow direction it has a 4 cm-wide uniform distribution with Gaussian edges (1-cm rms). These measures keep the peak power deposition in the jet below 0.7 MW/cm^2, less than that in FMIT. In the reference configuration, sketched in Fig. 2, the two lithium targets are oriented at 90° and spaced 30 cm from a common vertex. The jets are formed by nozzles into 2 cm thick ribbons flowing at 17.3 m/s along a concave steel back wall. A free surface faces the beam. The 35 MeV D^+ ions stop in the lithium jet, depositing most of their energy, but centrifugal pressure induced by the curved flow path prevents vapor formation. Thermal hydraulic simulations were done to confirm jet behavior, showing that the output lithium temperature (672° C) is less than that calculated for FMIT, because of the broad beam distribution.

Neutron flux volume and spectral properties in the test cell are determined by the beam distribution (in space and energy) within the target and by the dependence of the reaction cross sections on D^+ energy and neutron emission angle. The uncollided neutron flux at a grid of points in the test cell was computed by generating a differential cross section table from fits to existing Li(d,n) data, and then integrating over the D^+ energy loss function in the target and summing contributions from all parts of the two beam target interaction zone.[2] Calculated flux contours in the plane of the D^+ beams are shown in Fig. 3, using a conversion to equivalent 14.1 MeV neutron wall loading power for comparison with fusion reactor parameters (1.0 MW · m^{-2} = 1.42 · 10^{18} n · m^{-2} · s^{-1}).

Evident in the figure (reference case) are (1) large regions of low flux gradient and moderate flux levels in the center of the test cell, and (2) smaller regions (0.1 liter) with high wall loading and high flux gradient close to the targets. Comparison of this flux map with maps for other situations reveals that as the relative target angle increases, flux gradients are reduced and the test volume at medium to low flux levels increases.[2] Conversely, as the relative target angle decreases, flux gradients become steep, but the test volume at high wall loadings greatly increases. Gradients and

flux/volume relations can thus be tailored to suit specific user requirements by adjusting the relative target orientation and spacing.

Using the neutron flux grid, the useful volume enclosing regions of a specified average flux was calculated. The resulting flux-volume relations are displayed in Fig. 4 for several total currents. At the reference level (500 mA), a test volume of 10 liters can be achieved with average wall loadings up to 4 MW · m^{-2}. The flux volume relations at fixed current and volume-current relations at a fixed flux can be represented by simple exponential expressions. For example, at 5 MW · m^{-2} wall loading, the dependence on current is V(liters) = 28.0 I$^{1.8}$ (A), which explicitly reveals the strong advantage of scaling to higher D$^+$ currents.

Neutrons are generated in the lithium target primarily through the ^{6}Li(d,n)^{7}Be stripping reaction, with smaller contributions from other processes. The neutron angular distribution is forward peaked. A small fraction of the flux is in a high energy tail (up to 50 MeV) arising from the ^{7}Li(d,n)^{8}Be reaction. Details of the neutron spectrum depend on emission angle and distance from the target. At angles near 0° and locations away from the target, the stripping reaction dominates and there is a broad peak at 14 MeV, about half the beam energy. At large emission angles and locations close to the target, the spectrum contains a higher proportion of lower-energy (few MeV) evaporation neutrons. Figure 5 shows the uncollided flux as a function of energy at various positions (x,y,z) within the test cell. The x axis is along the beam, the y axis along the jet flow, and the z-axis transverse to the flow. Position (0,0,0) is the center of the target back plate the point of maximum flux. The high energy neutron tail is visible here, with about 15% of the neutrons having energies above 14 MeV. At other cell locations, the high energy portion of the spectrum is contain a fraction not larger than 20%. Preliminary analysis of damage data in copper[2] suggests that the gh energy tail should not significantly degrade the usefulness of the d Li source as a fusion damage simulator, but further evaluation is required to settle this issue.

Tritium-H_2O Neutron Source

In the High-Intensity 14 MeV Cutoff Neutron Source described in reference 4, neutron production is based on the ^{1}H(t,n)^{3}He reaction. Energetic tritium ion beams are injected into two hydrogenic targets in a geometry similar to that described for the d Li source. Tritium ions are accelerated in an RFQ/DTL accelerator similar to that described by Los Alamos for 250 mA deuterium beams.[3] The hydrogenic targets are provided by high velocity free water jets in which the beam deposited power can be absorbed without disruption of the flow if a suitable beam energy spread is provided. A typical beam target interaction region is sketched in Fig. 6. When the water jet targets are oriented at a relative angle of 120°, neutron fluxes · 10^{19} n · m^{-2} · s^{-1} can be achieved in a volume of 0.16 liters, and fluxes · 10^{18} n · m^{-2} · s^{-1} can be achieved in a volume of 4.2 liters. For a beam power of 17.5 MW, the corresponding values are 0.33 liters and 9.1 liters, respectively. The outstanding feature of this source is a high spectral intensity in the the energy range from 1 to 14 MeV with a sharp cutoff at an energy of 14.6 MeV

The global spectrum of this neutron source is shown in Fig. 7, where it is seen that the spectrum integrated over all angles from 0° to 67° is almost flat from ~1 to 14 MeV and exhibits a sharp energy cutoff level at 14.6 MeV.

Figure 8 shows a flux-contour map for a source configuration in which 250-mA T^+ beams are incident on two targets oriented at 120° and centered 8 cm from their common vertex. The assumed triton beam diameters are 4 cm, and the contour lines refer to regions enclosing the indicated average neutron flux levels. It can be seen that there are relatively large regions enclosing the indicated average neutron flux levels and also that there are relatively large regions with low flux gradients (i.e., between 0.5 and $2 \cdot 10^{18}$ $n \cdot m^{-2} \cdot s^{-1}$). This provides good irradiation of sample specimens in the form of long bars or rods at intermediate flux levels when small variations of flux levels over the whole sample are required. Close to the water targets there are two isolated regions with very high flux levels (> $1 \cdot 10^{19}$ $n \cdot m^{-2} \cdot s^{-1}$) but high flux gradients in which small materials specimens can be exposed. Similar calculations were performed for other relative target orientation angles and spacings [5]

Uncollided neutron flux spectra at the positions indicated in Fig. 8 were estimated by simple superposition of contributions from both target volumes to obtain the spectra shown in Fig. 9. Spectra for positions not too close to the targets extend to cutoff levels close to 14.6 MeV and typically show a broad flat top over several MeV at the upper end. Below the flat-top region the spectral intensity usually decreases rapidly with decreasing energy. The most suitable test cell regions to simulate first wall conditions of a fusion reactor are at positions 3 and 4 where fairly large samples can be irradiated at flux levels in the range of $1.3 \cdot 10^{18}$ $n \cdot m^{-2} \cdot s^{-1}$

Spallation Neutron Source

In spallation neutron sources, which are now in operation for materials research at several laboratories worldwide, neutrons are produced by the interaction of medium energy (500–1000 MeV) protons with heavy metal targets, such as lead, uranium, or tungsten. In the spallation process, illustrated in Fig. 10, each incident proton produces a shower of neutrons (and other particles) through an intranuclear and internuclear cascade process, followed by evaporation from residual excited nuclei. Proton currents at existing facilities are relatively modest (~100 μA), an international high flux source for fusion materials development would require about a factor of 50 more current. A source in this class, the SNQ facility, was proposed a few years ago in Germany and studied in considerable detail, but was not built.[6,7] Reference 8 provides a review of spallation source options and technology for a high flux source, and Reference 9 describes a proposed fusion materials spallation source based on a 600 MeV, 6 mA (average) proton beam incident on a flowing lead bismuth eutectic target.

Figure 11 shows the spallation neutron yield obtained in various target materials [10], as a function of proton energy and target diameter, and Fig. 12 shows the calculated neutron angular distribution from 800 MeV protons on a depleted uranium target. It can be seen that the neutrons with energies

> 10 MeV, which originate from the cascade processes, are forward peaked, with the peaking increasing with neutron energy, while the evaporation neutrons (< 10 MeV) are emitted more-or-less isotropically. In the forward direction the spectrum contains a very high energy tail, which can go all the way up to the full beam energy. This tail may be problematical for interpretation of damage information, but could in principle be reduced by neutron transport in the target material and in the materials immediately surrounding the target, and also by appropriate restriction of the specimen irradiation angles.

Several high-power target options have been considered for spallation sources, including rotating solid disks cooled by internal water channels,[7] and various kinds of liquid lead or lead/bismuth geometries and flow arrangements.[7,8] A group at IFN, Madrid [9], have studied a 600-MeV 6-mA spallation neutron source for fusion materials research in which the target consists of a stacked array of narrow (1 cm-wide) flowing lead-bismuth channels. Figure 13 indicates the geometry. The calculated neutron spectral distribution from this target is displayed in Fig. 15 for two distances from the beam axis, at a plane 3.75 m downstream from the target face. The flux at a radial distance of 1.3 cm is shown in Fig. 16 as a function of axial distance from the target face for several neutron energy groups. As seen in the figures, the flux levels desired for fusion materials testing can be attained but the extremely close proximity of the planned irradiation zones to the primary target may cause difficulties in terms of sample heating, bombardment by high-energy charged particles, and also sample placement and access.

The Madrid group [9] have proposed a 6 mA (average) current and 600 MeV proton energy as the appropriate beam specifications for driving a spallation fusion-materials neutron source. However, the optimum accelerator technology has not been decided. The two most likely possibilities are a pulsed linac or a multistage ring cyclotron. Comparative design studies and cost estimates will be needed to decide the issue. While the required beam performance would be straightforward for a linac, the capital costs would be high, and the facility would be much larger than either a d-Lithium or t-H$_2$O source. A ring cyclotron could be compact and possibly less expensive, but the desired beam current level may be difficult to achieve in this kind of machine.

Summary and Comparisons

Three kinds of accelerator driven neutron source have been proposed to meet the flux, volume and other test parameters desired for an international fusion materials research facility. The d-Lithium source concept is based on 35 MeV deuterons incident on liquid lithium, and has its origins in the FMIT project pursued in the early 1980s. The required high power cw deuteron linac is feasible, and the design approach is supported by a solid technology base developed, in part, through the SDI Neutral Particle Beam program. The lithium target technology was tested at high power levels during the FMIT program, although not with an incident beam. The proposed d-Lithium source could be built now, but there is some concern about the effects of the high energy neutron spectral tail on interpretation of materials damage data.

The t-H_2O source is a recent suggestion, with triton beams substituted for deuterons, and water substituted for lithium. The attraction is the possibility of eliminating the problematical high-energy tail that occurs in the d-Lithium reactions, but the technology is more challenging than for the d-Lithium source and is not developed. A high-power triton linac is feasible. (with somewhat lower current limits than in the deuteron case), but tritium contamination of the accelerator would be an issue in terms of additional maintenance requirements. The water jet concept has not been tested in the required performance range, which is very challenging. While preliminary scoping calculations are encouraging, there may be power deposition limitations, and also nozzzle erosion problems due to the high fluid velocity. Tritium extraction from the water system will be expensive, adding significantly to the facility cost, and the effort to obtain facility licencing would almost certainly have an impact on the implementation schedule. Finally, the flux-volume product for the t-H_2O source may be a factor of 2 to 3 less than that for the d-Li source at the same level of beam power.

The spallation source produces neutrons more economically (in terms of electric power costs) than the d-Li or t-H_2O sources, but capital costs would be much higher if a linac is required as the driving accelerator. If cyclotron technology is feasible for the driver, then capital cost may be similar to the other sources. The neutron spectrum is initally a poor match to the desired first wall spectrum, and has a very high energy tail. In principle the spectrum could be tailored adquately by placement of appropriate materials adjacent to the production target, but feasibility has not been shown. Because of the central target location with respect to the test zone, high flux gradients seem unavoidable, and because of the high beam energy there will be high energy protons and other unwanted particles showering the test samples. To attain the desired neutron flux levels, it is necessary to place samples very close to the neutron production target, with attendant problems of sample heating, placement, and access.

Table 1. Parameters for D-Lithium Source Driver

Accelerator	RFQ	DTL
Deuteron energy (MeV)	3.0	35 - 40
Beam current (mA)	125	250
Linac length (m)	5.4	16.3
Accel. field, E_0T (MV/m)		2.0 - 2.5
Aperture radius (mm)	6.0	9.0
RMS beam size (mm)	1.5	1.4
Output emittance (n,RMS)		
Trans. (π mm-mrad)	0.27	0.34
Long. (π mm-mrad)	0.46	0.52
RF Power (MW)		
Structure	0.3x2	3.0
Beam	0.4x2	8.0
Total	1.4	11.0
Beam at Target		
Energy spread, RMS (MeV)	± 1.0	
Beam dimensions at target (cm)		
Along lithium flow (Gaussian, RMS)	± 1.0	
Transverse to flow (Rectangular)	± 2.0	
Lithium Jet Target		
Avg. jet thickness (mm)	20.5	
Flow velocity (m/s)	17.3	
Max. energy deposition (MeV/mm)	4.6	
Peak current density (mA/cm^2)	15.4	
Peak power density (MW/cm^3)	0.7	
Input lithium temperature (°C)	220	
Max. lithium temperature (°C)	672	
Min. boiling margin (°C)	466	
Surface evaporation (g/s)	6.4×10^{-5}	

References

1. D. G. Doran and J. E. Leiss, "Neutron Source Evaluation Process and Evaluation Panel Report," J. of Fusion Energy, **8**, 3/4, 137-141 (1989).

2. G. L. Varsamis, G. P. Lawrence, T. S. Bhatia, B. Blind, F. W. Guy, R. A. Krakowski, G. H. Neuschaefer, N. M. Schnurr, S. O. Schriber, T. P. Wangler, and M. T. Wilson, "Conceptual Design of a High-Performance Deuterium-Lithium Neutron Source for Fusion Materials and Technology Testing, " Nucl. Sci. and Eng., **106**, 160-82 (1990).

3. T. L. Trego, J. W. Hagan, E. K. Opperman, and R. J. Burke, "Fusion Materials Irradiation Test Facility--A Facility for Fusion Materials Qualification," Nuclear Technology/Fusion, **4** (2) Part 2, 695 (1983).

4. S. Cierjacks, Y. Hino, and M. Drosg, "Proposal for a High-Intensity 14 MeV Cut-off Neutron Source Based on the $^{1}H(t,n)^{3}He$ Source Reaction," Nucl. Sci. and Eng., **106**, 183 (1990).

5. S. Cierjacks and Y. Hino, "Additional "Studies Related to the Proposal for a Novel High-Intensity 14-MeV Cutoff Neutron Source Based on the $^{1}H(t,n)^{3}He$ Source Reaction," Proc. International Panel on 14-MeV Intense Neutron Sources Based on Accelerators for Fusion Materials Study, Tokyo, Report NIFS-WS-2 (January, 1989).

6. G. Bauer, et al., "International Report of the SNQ-Project," Nr. SNQ 1 HG/BH001 KFA Julich (1982).

7. G. Bauer, et al., "Realizierungsstudie zur Spallations Neutronenquelle," Jul-Spez 113, KfK Karlsruhe 3175 (1981).

8. G. Bauer, "Spallation Neutron Sources: Basics, State of the Art, and Options for Future Development," J. of Fusion Energy, **8** (3/4), 169-180 (1989).

9. J. Perlardo, M. Piera, and J. Sanz, "Option for Spallation Neutron Source," J. Fusion Energy, **8** (3/4), 181-192 (1989).

10. Fraser, et al., "Neutron Production in Thick Targets Bombarded by High Energy Protons," Phys. Canada, **21**, 17-18 (1965).

11. G. Russell, "Parametric Studies of Target/Moderator Configurations for the Weapons Neutron Research (WNR) Facility (1977).

Figure Captions

Fig. 1. Reference D-Li neutron source: two 250-mA modules and two targets. Lightly-drawn modules indicate upgrade path (from Varsamis [2]).

Fig. 2. Schematic of target and test zone for D-Lithium source (from Varsamis [2]).

Fig. 3. Neutron flux (wall-loading power) contours for two 250 mA beams: relative target orientation 90° (from Varsamis [2]).

Fig. 4. Test volume vs. uncollided neutron wall-loading power as a function of total beam current (from Varsamis [2]).

Fig. 5. Uncollided neutron flux as a function of energy for several points within the test region (from Varsamis [2]).

Fig. 6. Schematic of beam-target interaction for t-H_2O source (from Cierjacks [4]).

Fig. 7 14-MeV cutoff neutron source global neutron spectrum, integrated from 0° to 67° (from Cierjacks [4]).

Fig 8. 14-MeV cutoff neutron source neutron flux contours (from Cierjacks [4]).

Fig. 9. 14-MeV cutoff neutron source primary neutron energy spectra at positions indicated in Fig 8 (from Cierjacks [4]).

Fig. 10. Spallation neutron production process.

Fig. 11. Neutron yield in various target materials (from Fraser [10]).

Fig. 12. Calculated neutron angular distribution from 800-MeV protons on a depleted uranium target (from Russell [11]).

Fig. 13. Conceptual design of the flowing liquid lead-bismuth target proposed for high-power spallation source (from Perlardo [9]).

Fig. 14. Irradiation zones perpendicular to the beam axis for target geometry of Fig. 13 (from Perlardo [9]).

Fig. 15. Neutron spectra at 3.75 cm from target face for two radial positions, 1.3 cm and 2.0 cm (from Perlardo [9]).

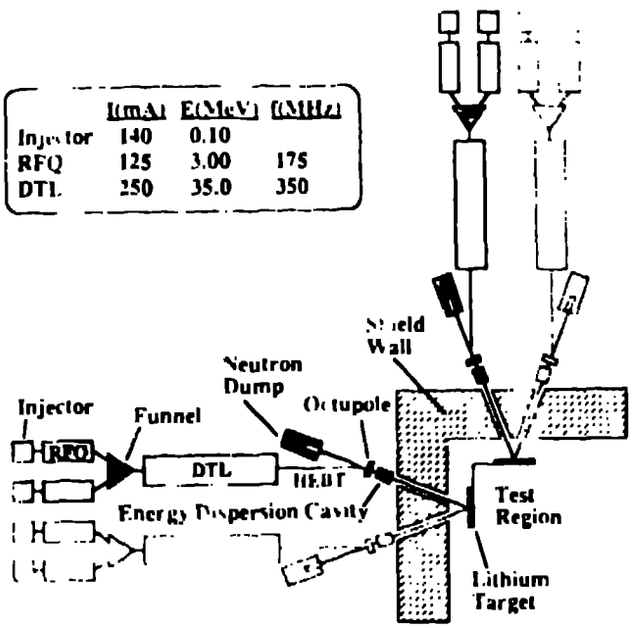
I(mA) E(MeV) f(MHz)
Injector 140 0.10
RFQ 125 3.00 175
DTL 250 35.0 350
Shield Wall
Neutron Dump
Octupole
Injector
Funnel
RFQ
DTL
HEBT
Energy Dispersion Cavity
Test Region
Lithium Target

Fig. 1

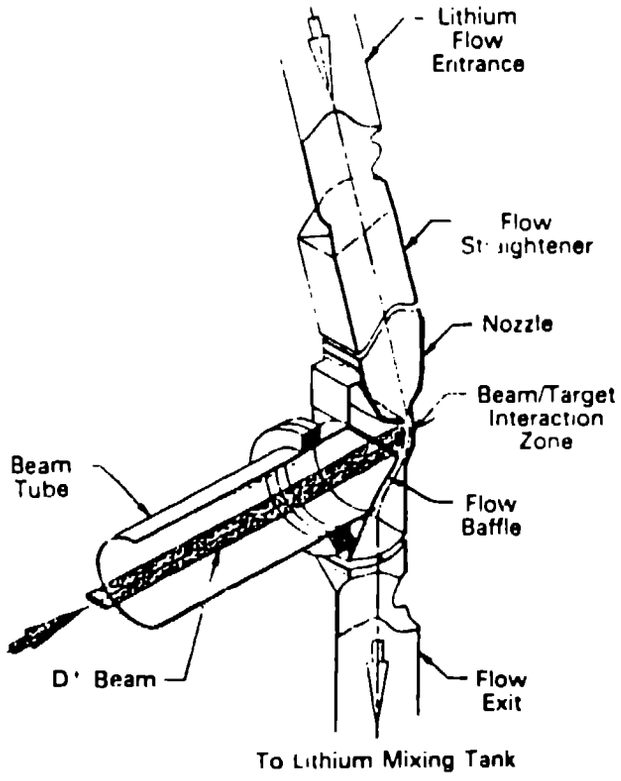
Lithium
Flow
Entrance
Flow
Straightener
Nozzle
Beam/Target
Interaction
Zone
Beam
Tube
Flow
Baffle
D+ Beam
Flow
Exit
To Lithium Mixing Tank

Fig. 2

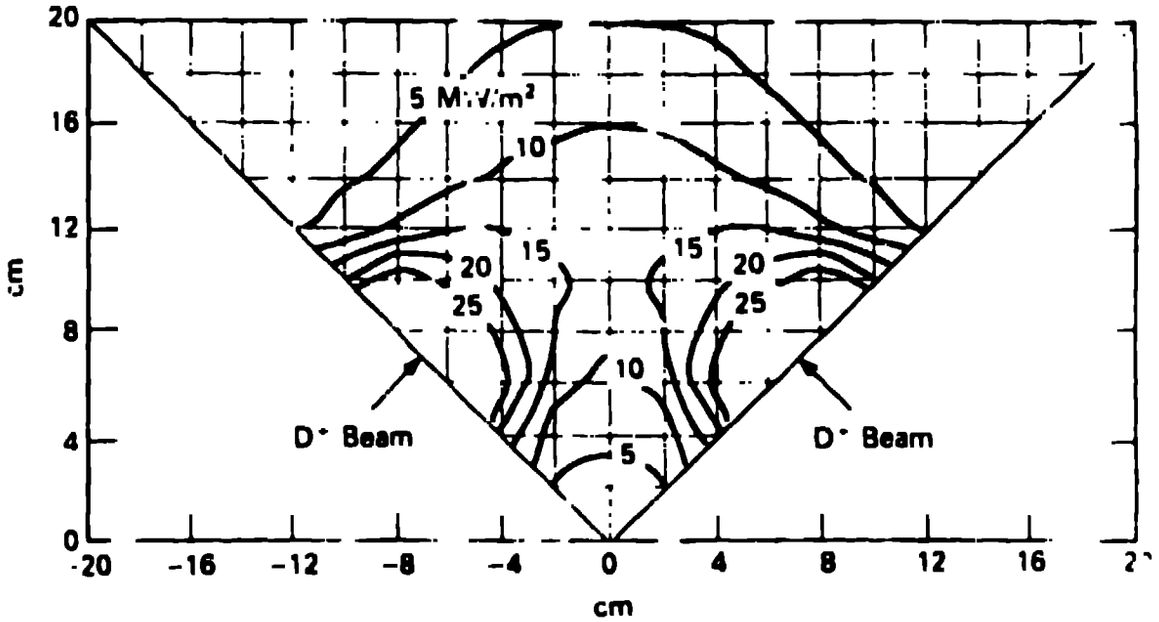
20
16
12
8
4
0
cm
-20
-16
-12
-8
-4
0
4
8
12
16
5 MV/m²
10
15
20
25
15
20
25
10
5
D° Beam
D° Beam

Fig 3

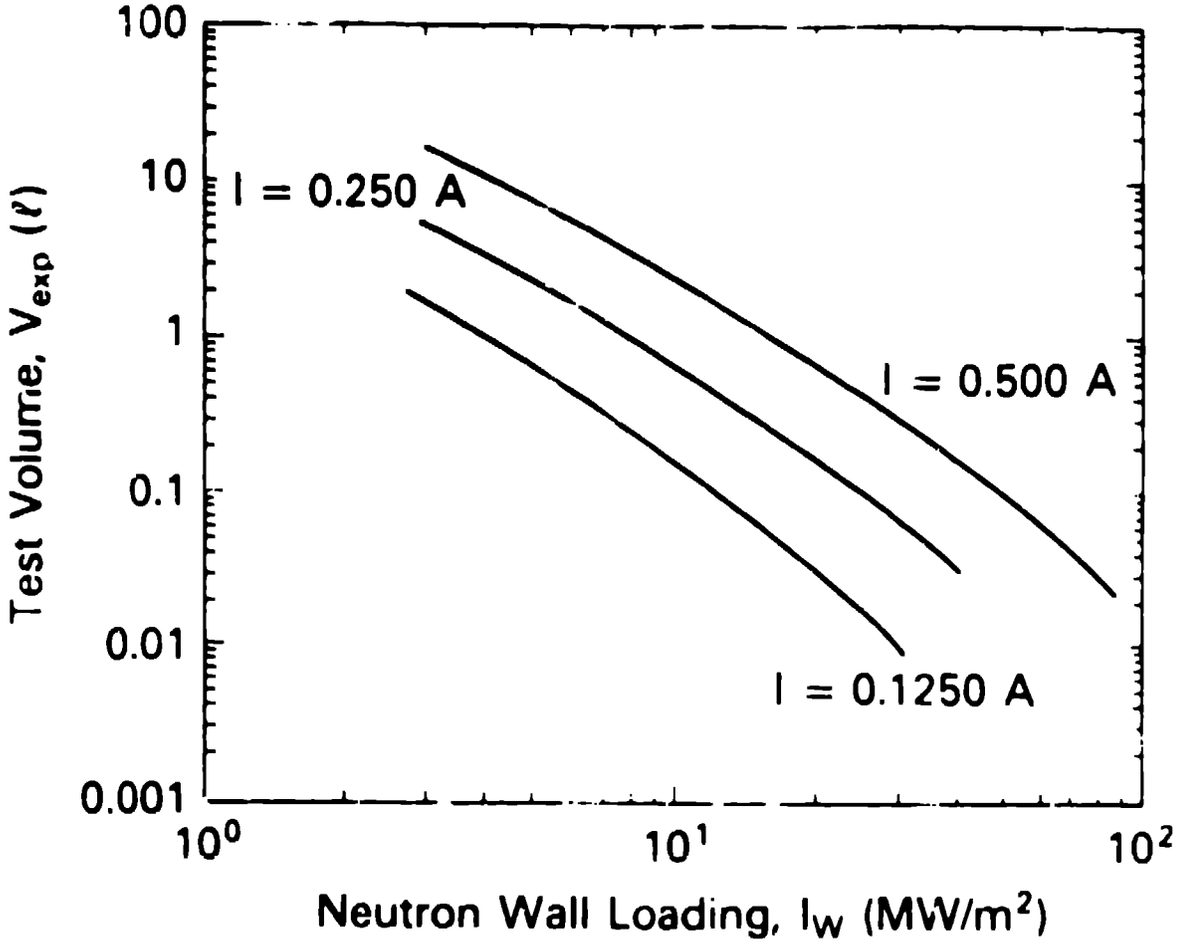
100
10
1
0.1
0.01
0.001
Test Volume, V_{exp} (ℓ)
I = 0.250 A
I = 0.500 A
I = 0.1250 A
10^0
10^1
10^2
Neutron Wall Loading, I_W (MW/m^2)

Fig. 1

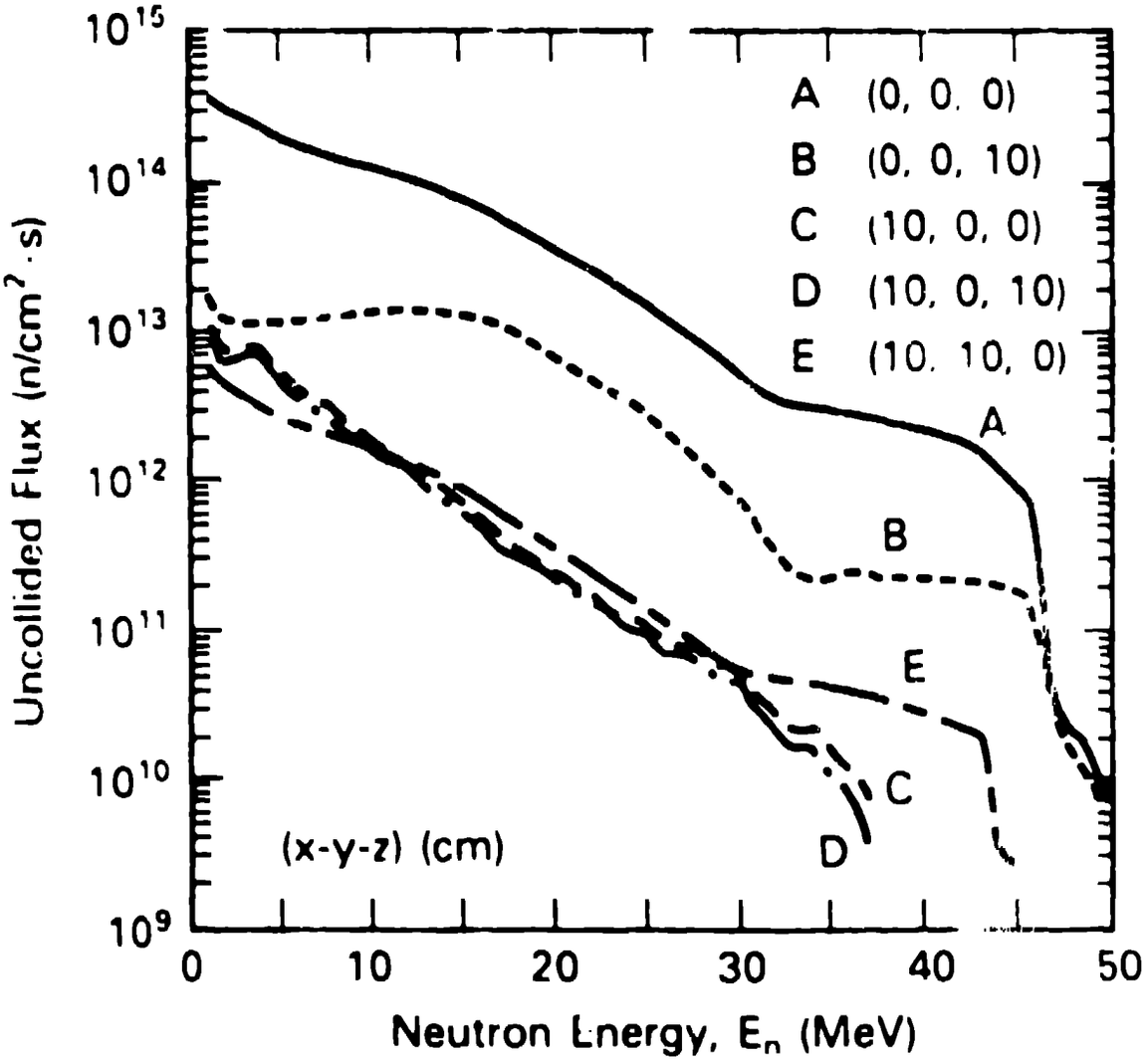
A (0, 0, 0)
B (0, 0, 10)
C (10, 0, 0)
D (10, 0, 10)
E (10, 10, 0)
A
B
C
D
E
(x-y-z) (cm)
Uncollided Flux (n/cm^2·s)
10^{15}
10^{14}
10^{13}
10^{12}
10^{11}
10^{10}
10^{9}
0
10
20
30
40
50
Neutron Energy, E_n (MeV)

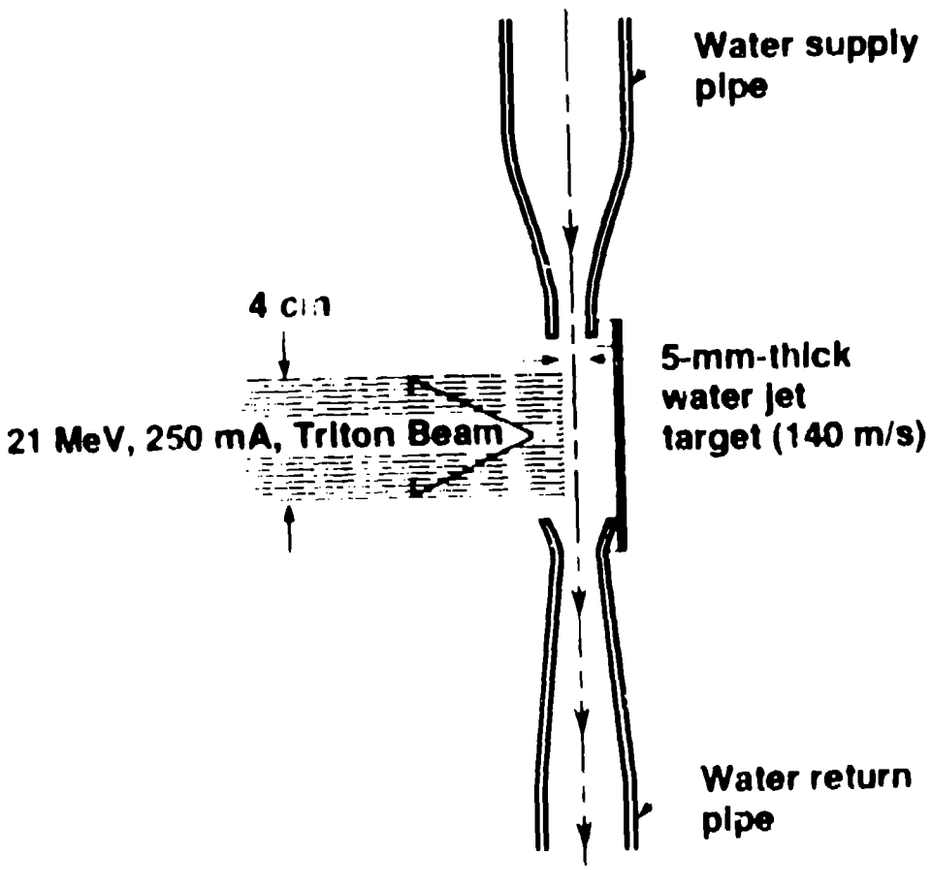
Water supply pipe
4 cm
5-mm-thick water jet target (140 m/s)
21 MeV, 250 mA, Triton Beam
Water return pipe

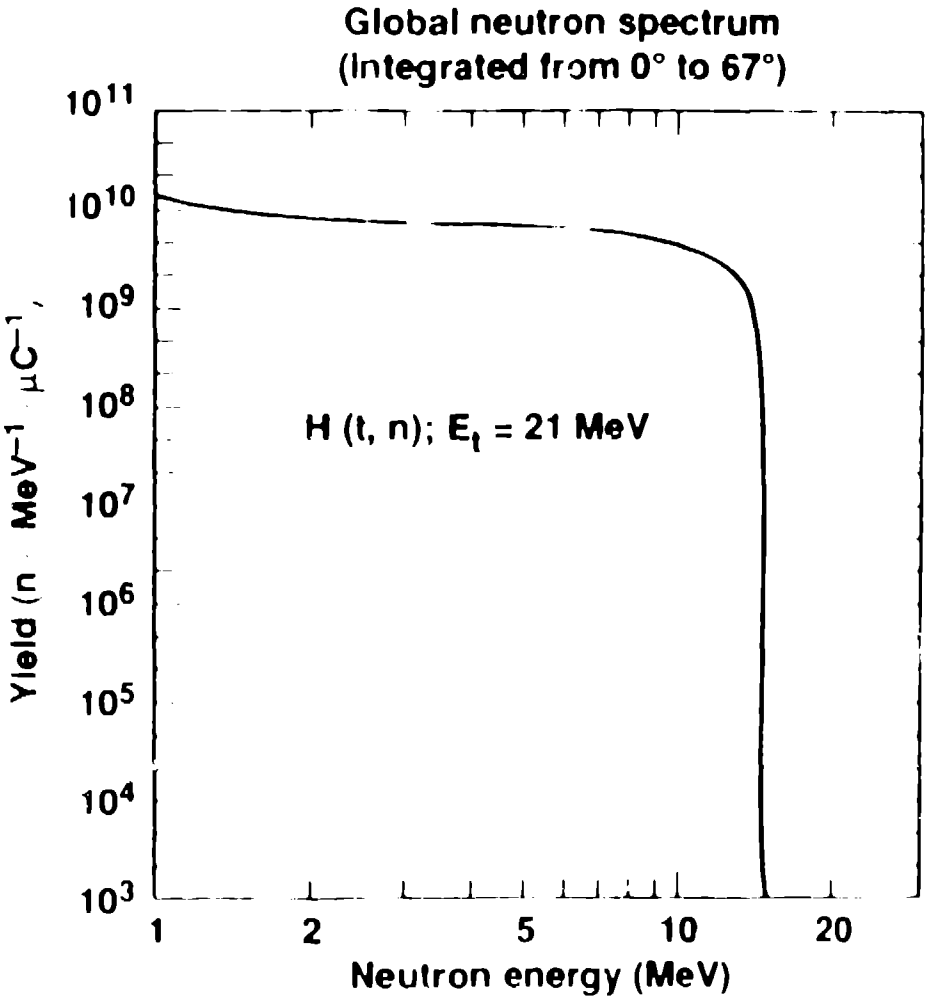
Global neutron spectrum
(Integrated from 0° to 67°)
10^{11}
10^{10}
10^{9}
10^{8}
10^{7}
10^{6}
10^{5}
10^{4}
10^{3}
Yield (n · MeV^{-1} · μC^{-1})
H (t, n); E_t = 21 MeV
1
2
5
10
20
Neutron energy (MeV)

Neutron Flux Contours

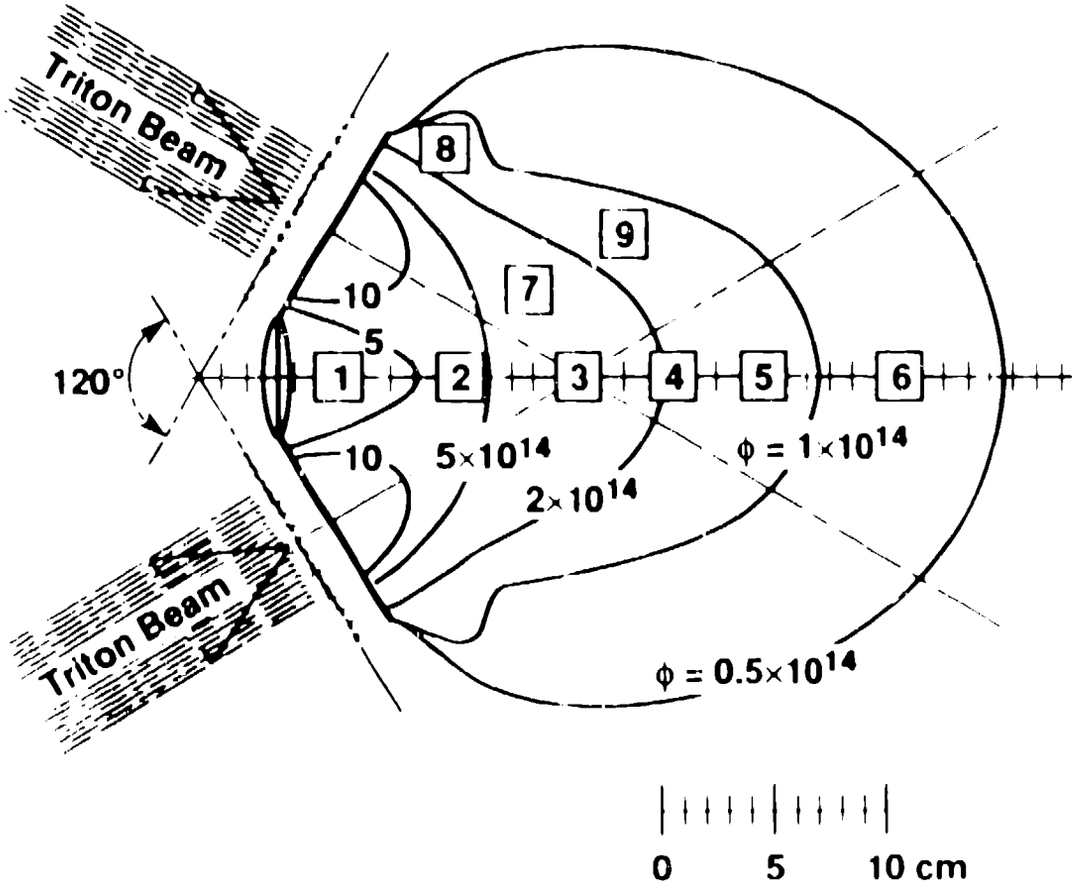

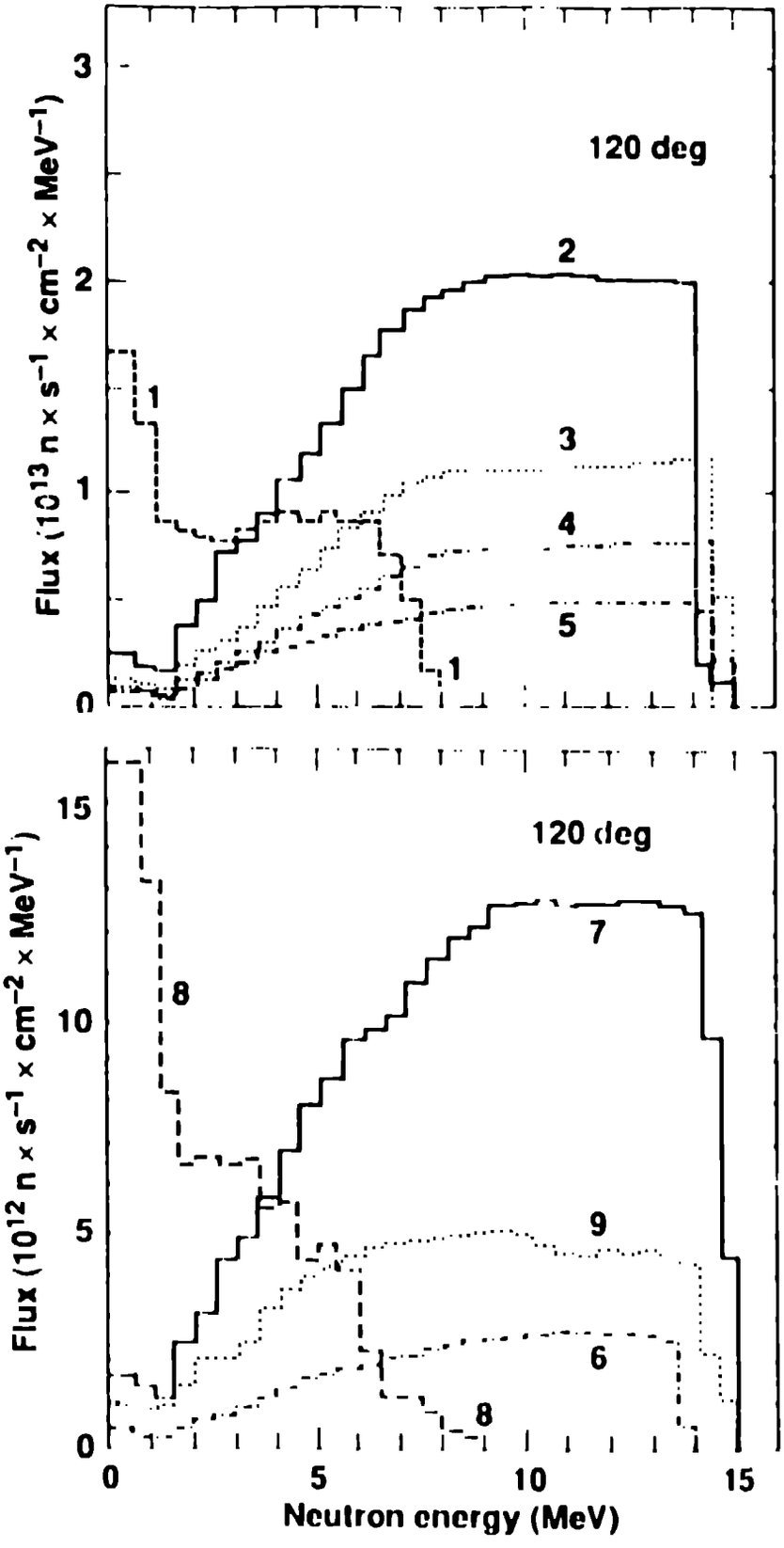
120 deg
Flux (10^{13} n × s^{-1} × cm^{-2} × MeV^{-1})
1
2
3
4
5
120 deg
Flux (10^{12} n × s^{-1} × cm^{-2} × MeV^{-1})
7
8
9
6
0
5
10
15
Neutron energy (MeV)

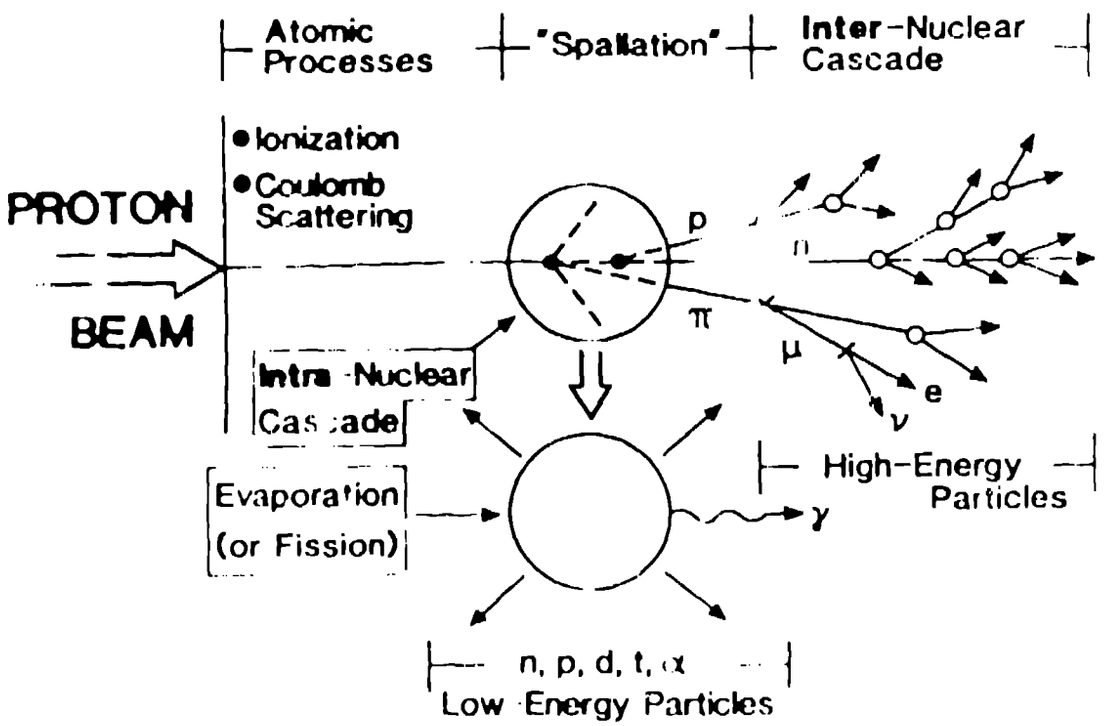
Atomic Processes
"Spallation"
Inter-Nuclear Cascade
PROTON BEAM
Ionization
Coulomb Scattering
p
π
μ
e
ν
n
Intra-Nuclear Cascade
Evaporation (or Fission)
γ
High-Energy Particles
n, p, d, t, α
Low-Energy Particles

Fig. 10

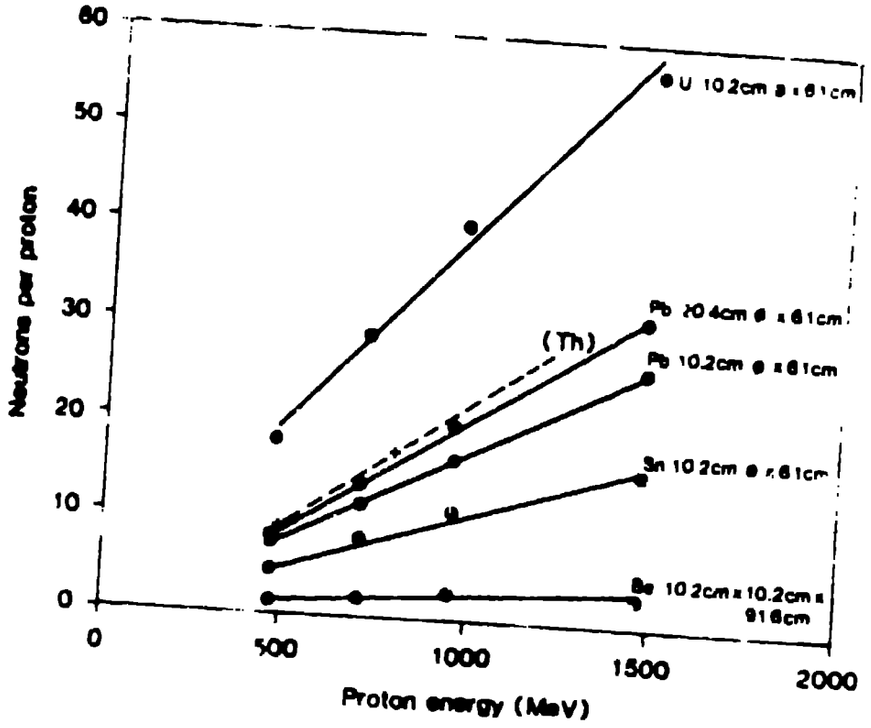
60
50
40
30
20
10
0
Neutrons per proton
0
500
1000
1500
2000
Proton energy (MeV)
U 10.2cm ø x 61cm
Pb 20.4cm ø x 61cm
(Th)
Pb 10.2cm ø x 61cm
Sn 10.2cm ø x 61cm
Be 10.2cm x 10.2cm x 91.6cm

Fig. 11

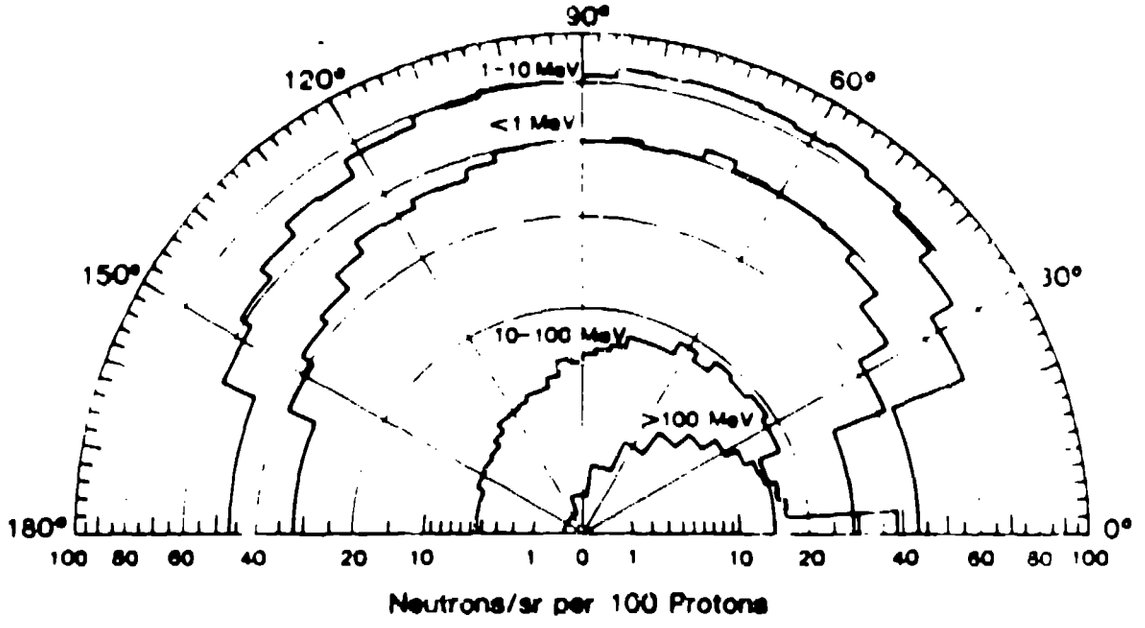
90°
120°
60°
150°
30°
180°
0°
1-10 MeV
<1 MeV
10-100 MeV
>100 MeV
100 80 60 40 20 10 1 0 1 10 20 40 60 80 100
Neutrons/sr per 100 Protons

Fig. 12.

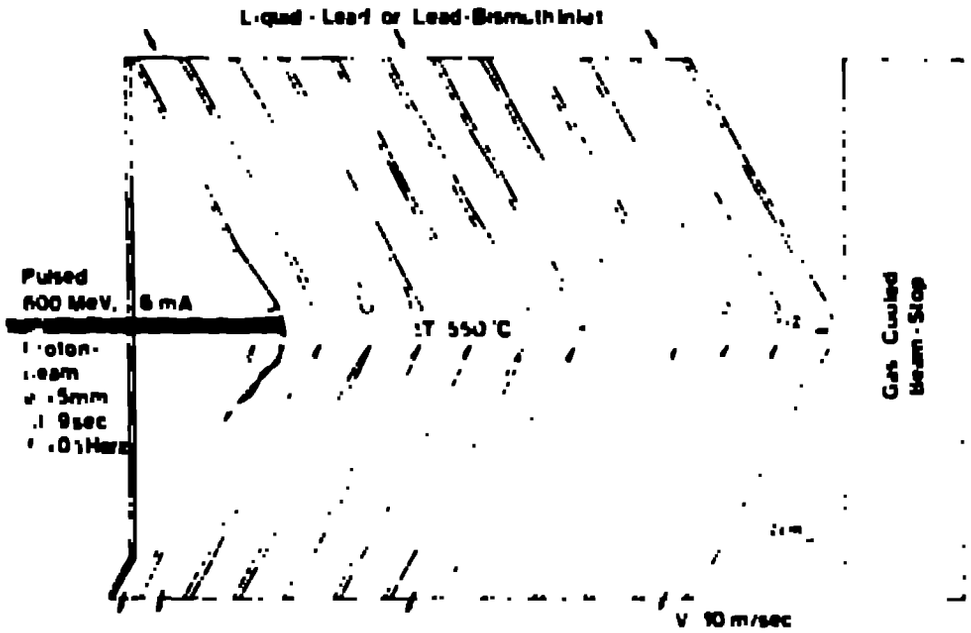
Liquid - Lead or Lead-Bismuth inlet
Pulsed
600 MeV.
6 mA
Proton-
beam
Gas Cooled
Beam-Stop
V 10 m/sec

Fig. 13

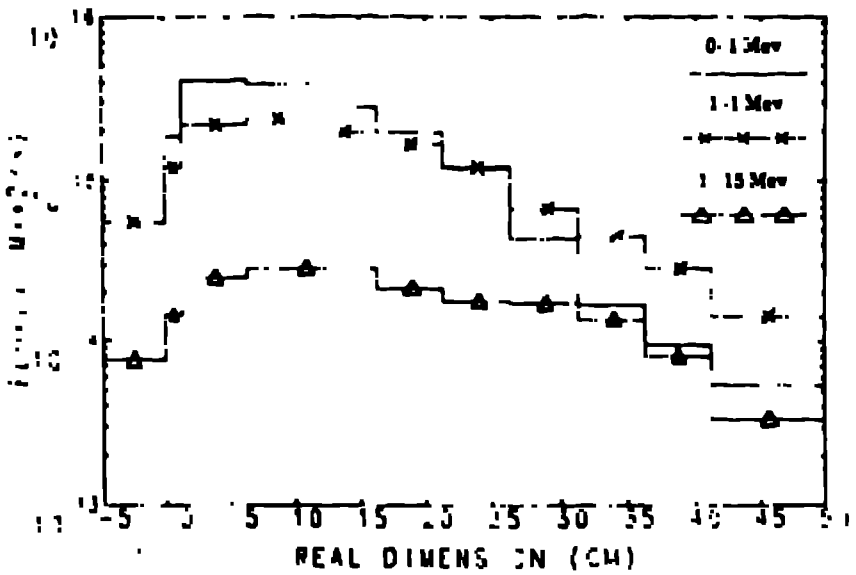
0-1 Mev
1-1 Mev
1-15 Mev
-5
0
5
10
15
20
25
30
35
40
45
50
REAL DIMENSION (CM)

Fig. 19

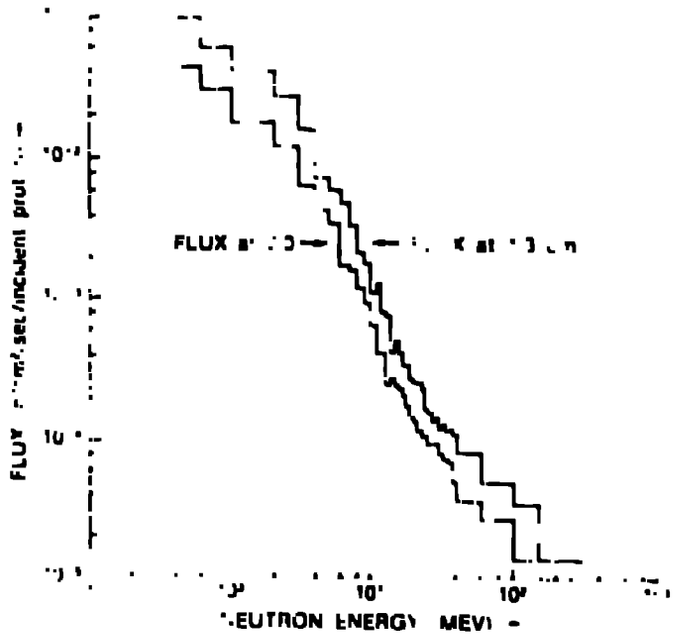

Fig. 15